



# ATLAS PUB Note

GROUP-2019-XX

27th September 2019



Draft version 0.1

1

2

## Comparison of $t\bar{t}+b\bar{b}$ and $t\bar{t}+V$ background samples for $t\bar{t}H$ analyses

3

4

The ATLAS Collaboration

5

This note presents Monte Carlo generator comparisons of the  $t\bar{t}+b\bar{b}$  and  $t\bar{t}+V$  processes at particle level. The aim is to compare the modelling of some important backgrounds and the treatment of the associated theory uncertainties for a full Run-2 ATLAS+CMS combination. As a first step, pre-fit modelling and theory uncertainties as used in the experiments are compared in the relevant analysis regions.

6

7

8

9

12
**Contents**

13	<b>1</b>	<b>Introduction</b>	<b>3</b>
14	<b>2</b>	<b>ttbb</b>	<b>4</b>
15	2.1	Samples	4
16	2.2	Fiducial Volume	4
17	2.3	Results	5
18	<b>3</b>	<b>ttV</b>	<b>9</b>
19	3.1	Samples	9
20	3.2	Fiducial Volume	9
21	3.3	Results	10

## 1 Introduction

The search for Higgs boson production in association with a top quark pair ( $t\bar{t}H$ ) in the  $H \rightarrow b\bar{b}$  [1] and  $H \rightarrow \text{multi-lepton}$  [2] final states is limited by the modelling uncertainties of the main backgrounds,  $t\bar{t}+b\bar{b}$  and  $t\bar{t}+V$  respectively, where  $V$  denotes either a  $W$  or  $Z$  boson. Examples of tree-level diagrams of said processes are shown in Figure 1. A comparison of available Monte Carlo generators is thus performed to study the modelling of important  $t\bar{t}H$  backgrounds and the associated theory uncertainties for a full Run-2 ATLAS+CMS combination. Here, comparisons of particle level observables are made, in a phase space similar to the reference measurements. The goal is to decide on a common strategy between ATLAS and CMS for background modelling uncertainties in the  $t\bar{t}H(b\bar{b})$  and  $t\bar{t}H(\text{multi-lepton})$  analyses.

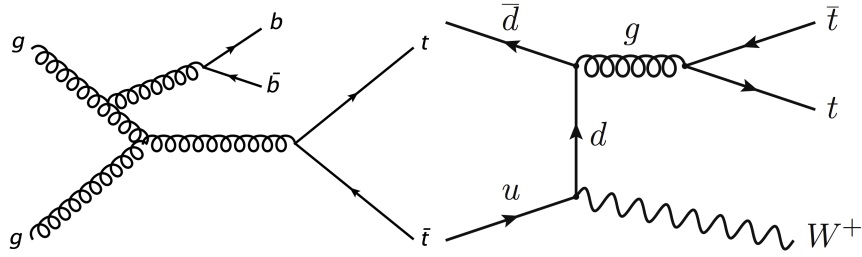


Figure 1: Examples of tree-level Feynman diagrams for  $t\bar{t}+b\bar{b}$  (left) and  $t\bar{t}+W$  (right).

## 2 ttbb

### 2.1 Samples

Four MC generators are compared in this study, where the inclusive  $t\bar{t}$  PP8 sample was previously used as the nominal background estimate in the ttH analysis. It is generated with the POWHEG-BOX v2 NLO event generator [3–6] with NNPDF3.0 NLO PDF set, matched to Pythia8 and is referred to as PP8  $t\bar{t}$ , where the additional bb-pair is described by the parton shower. The  $h_{damp}$  parameter was set to 1.5 times the top quark mass [7], which is assumed to be 172.5 GeV. The parton shower and the hadronisation were modelled by Pythia 8.210 with the A14 set of tuned parameters. The renormalisation and factorisation scales were set to the transverse mass of the top quark. The intrinsic uncertainty of the nominal PP8  $t\bar{t}$  sample is expressed by the simultaneous variation of the renormalisation and factorisation scales together with the PDF tune parameter. The RadiationUp variation has the renormalisation and factorisation scales decreased by a factor of two, the Var3c upward variation of the A14 parameter set and the  $h_{damp}$  parameter doubled. The RadiationDown variation has the renormalisation and factorisation scales increased by a factor of two, the Var3c downward variation and the nominal value of  $h_{damp}$ . Additionally, the up and down radiation uncertainty is calculated following the CMS approach, under which the renormalisation scale, factorisation scale and PDF tune variations are each taken individually and their difference to the nominal is summed in quadrature.

The PP8 tt+bb sample also uses the POWHEG generator where  $t\bar{t}b\bar{b}$  matrix elements are calculated at NLO with massive b-quarks, using the four-flavour NLO NNPDF3.0 PDF set [8]. The parton shower and hadronisation is modelled by Pythia 8.240.

For the PP8 samples the bottom and charm quark decays are described by EVTGEN v1.2 [9] and the top quark spin correlations follow reference [10].

The SHERPA tt+bb sample describes NLO tt+bb including parton showering and hadronisation by SHERPA-OPENLOOPS [11–13]. The sample was produced with Sherpa version 2.1.1 and the CT10 four-flavour scheme PDF set [14, 15]. The renormalisation scale is set to the CMMPS value as in ref [11], the factorisation and resummation scales equal  $H_T/2$ .

Both the PP8 tt+bb and the SHERPA tt+bb samples describe the additional bb-pair with NLO precision in QCD, taking into account the b-quark mass

The SHERPA  $t\bar{t}$  sample uses SHERPA version 2.2.1 [12] with the ME+PS@NLO (multi-leg) setup using the MEPS@NLO prescription [16], interfaced with OPENLOOPS. It provides NLO accuracy for up to one additional parton and LO accuracy for up to four additional partons. The NNPDF3.0 NNLO PDF set is used with a five-flavour scheme and both renormalisation and factorisation scales are set to  $\sqrt{0.5 \times (m_{T,t}^2 + m_{T,\bar{t}}^2)}$ . A summary of all samples used is given in Table 1.

### 2.2 Fiducial Volume

Object and event selection is defined at particle-level that closely matches the detector-level described in reference [1]. Jets are reconstructed from stable particles with a mean lifetime of  $\tau > 3 \times 10^{-11}$  s, using the anti- $k_t$  algorithm with a radius parameter of  $R = 0.4$ , and are required to have  $p_T > 25$  GeV and  $|\eta| < 2.5$ . Jets are matched to b-hadrons with  $p_T > 5$  GeV by ghost matching [17] and are referred to as

Table 1: The configurations used for the event generation of ttbb processes.

Process	Generator	ME order	Parton shower	PDF	Tune
$t\bar{t}$	PowHEG v2	NLO	PYTHIA 8	5FS NNP3.0 NNLO	A14
$t\bar{t} + b\bar{b}$	PowHEG v2	NLO	PYTHIA 8	4FS NNP3.0 NNLO	A14
$t\bar{t} + b\bar{b}$	SHERPA 2.1.1	NLO	SHERPA	4FS NNP3.0 NNLO	SHERPA default
$t\bar{t}$	SHERPA 2.2.1	ME+PS@NLO	SHERPA	5FS NNP3.0 NNLO	SHERPA default

b-jets. Electrons and muons, referred to as leptons, are required to satisfy  $p_T > 27\text{GeV}$ . Selected leptons are required to be separated from selected jets by  $\Delta R > 0.4$ . Events are selected with exactly one lepton and at least 4 jets, targeting the semi-leptonic  $t\bar{t}$  decay. Two regions are considered, defined by 3 b-jets or  $\geq 4$  b-jets.

### 2.3 Results

The nominal PP8  $t\bar{t}$  sample is compared to its radiation uncertainty variations and alternative generators, scaled to a common arbitrary integrated luminosity. The first ratio plot shows the ratio of the different MC samples to PP8  $t\bar{t}$ , where the colour scheme is given in the legend. Discrepancies between PP8  $t\bar{t}$  and the alternative generators can be seen in the  $\Delta R$  quantities, as in Figures 2 and 3, where at least in the 4b selection the difference to the alternative generators is larger than the uncertainty band given by the radiation variations. Interesting differences are also observed in the  $H_T$  distributions, particularly in the 3b selection, as illustrated in Figures 4 and 5. The jet multiplicity, as in Figure 6, has poor agreement among the generators for large jet multiplicities.

The second ratio plot shows the relative uncertainty of the radiation variations, shown as the ratio of the uncertainty to the nominal for three cases. The PP8  $t\bar{t}$  sample (black) and the PP8 tt+bb sample (blue), following the above description. It can be seen that this type of uncertainties is larger for the tt+bb case than in the  $t\bar{t}$  calculation. Also, the sum of individual variations following the CMS approach (red) on PP8  $t\bar{t}$  leads to a smaller uncertainty with respect to the simultaneous variation.

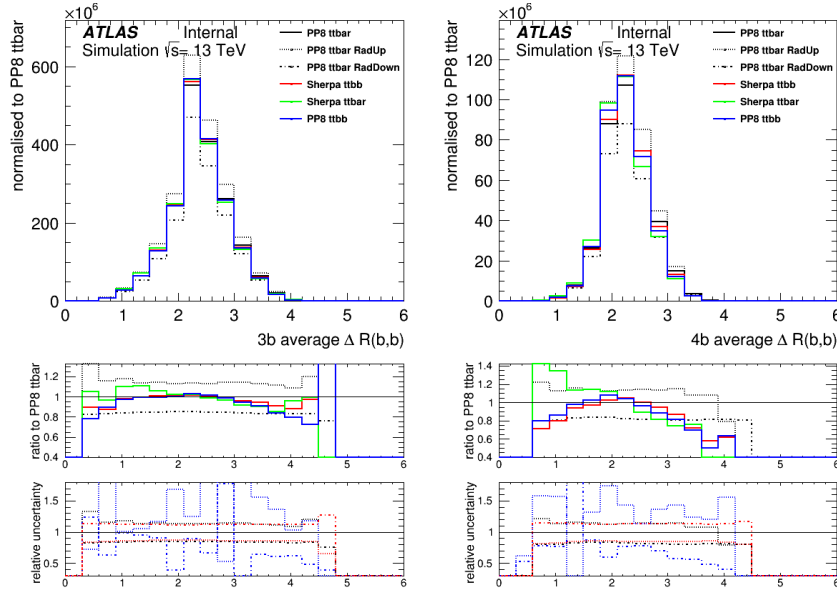


Figure 2: Distribution of the average opening angle between two b-jets, for the 3b selection (left) and the 4b-jet selection (right). Explanation in text.

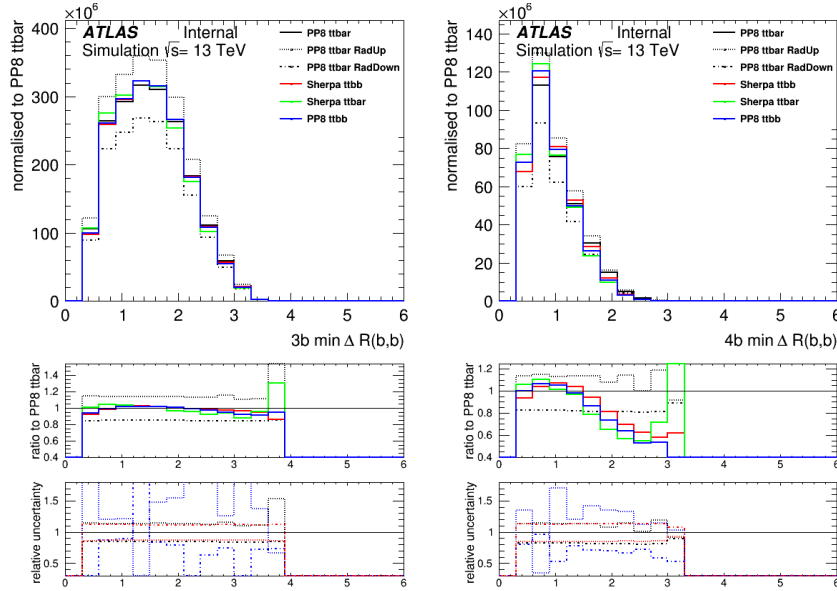


Figure 3: Distribution of the smallest opening angle between two b-jets, for the 3b selection (left) and the 4b-jet selection (right). Explanation in text.

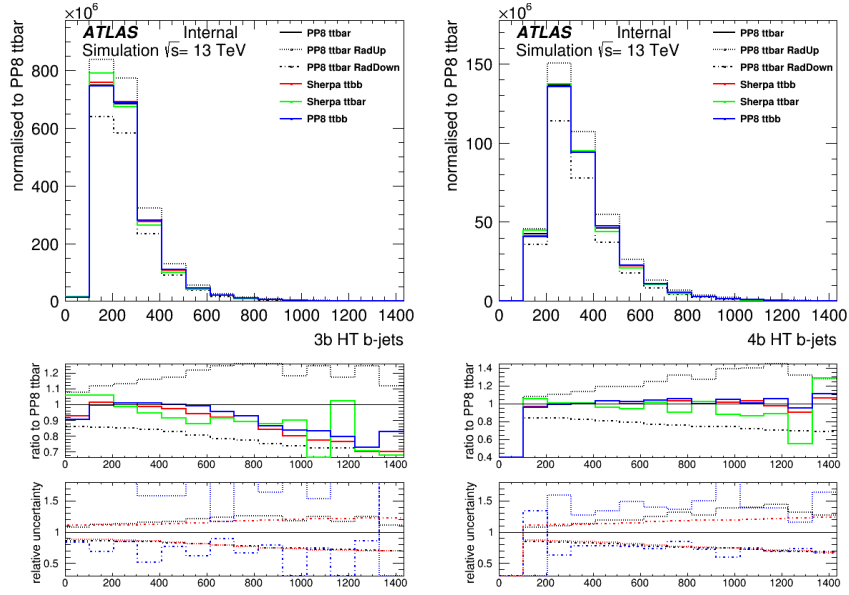


Figure 4: Sum of b-jet transverse momenta, for the 3b selection (left) and the 4b-jet selection (right). Explanation in text.

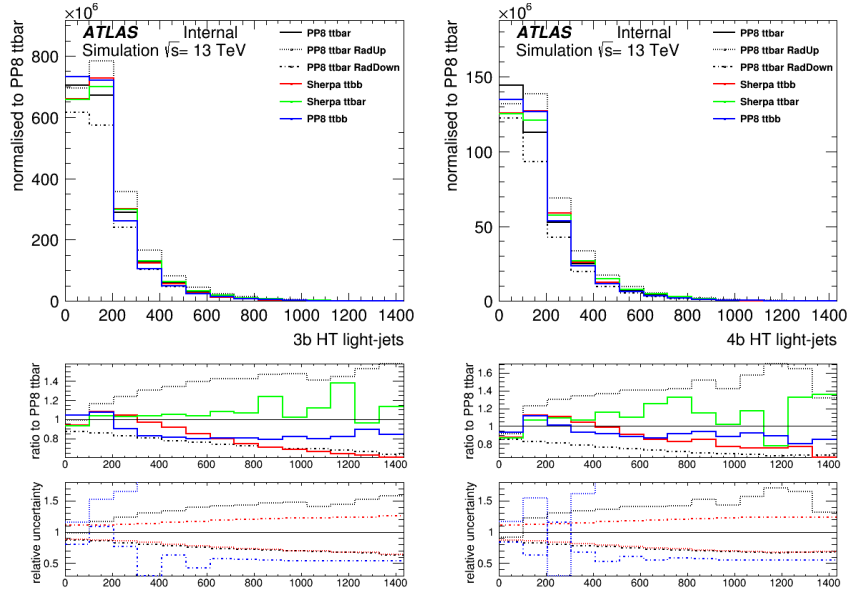


Figure 5: Sum of non-b-jet transverse momenta, for the 3b selection (left) and the 4b-jet selection (right). Explanation in text.

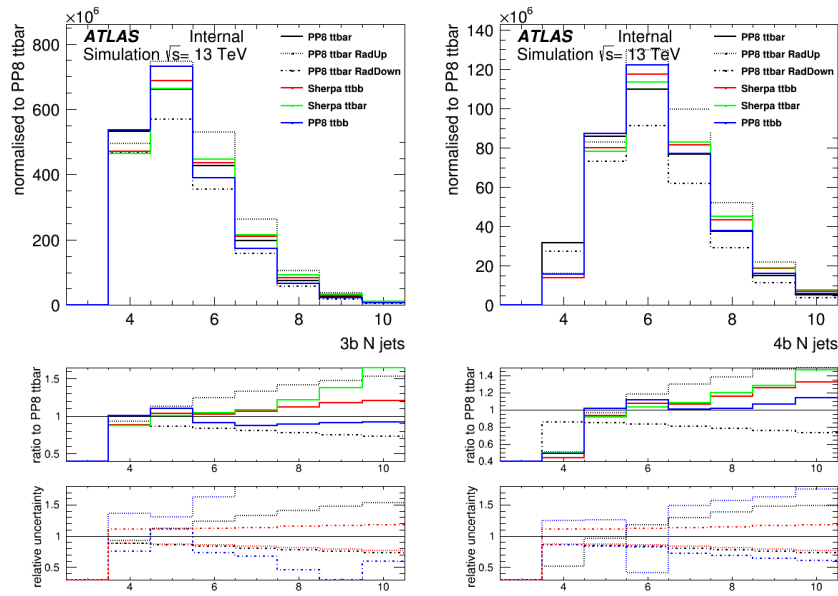


Figure 6: Jet multiplicity, for the 3b selection (left) and the 4b-jet selection (right). Explanation in text.



Table 2: The configurations used for the event generation of  $t\bar{t}W$  processes.

Process	Generator	ME order	Parton shower	PDF	Tune
$t\bar{t}W$	SHERPA 2.2.1	MEPs@NLO	SHERPA	NNPDF3.0 NNLO	SHERPA default
	MG5_AMC	NLO	PYTHIA 8	NNPDF3.0 NLO	A14

### 3 $t\bar{t}V$

#### 3.1 Samples

Two MC generators are compared in this study. The nominal sample for  $t\bar{t}W$  production was generated using the SHERPA 2.2.1 [18] generator with the NNPDF3.0 NLO PDF set. The matrix element (ME) was calculated for up to one additional parton at NLO and up to two partons at LO using COMIX [19] and OPENLOOPS [13], and merged with the SHERPA parton shower [20] using the MEPs@NLO prescription [16]. The choice of renormalisation and factorisation scales is  $\mu_R = \mu_F = H_T/2$ , where  $H_T$  is defined as the scalar sum of the transverse masses  $\sqrt{p_T^2 + m^2}$  of all final state particles.

Systematic uncertainties due to missing higher-order QCD corrections are estimated by varying the factorisation and renormalisation scales in the nominal sample simultaneously by a factor of 0.5 and 2.0 with respect to the central value. Uncertainties associated with the modelling of additional QCD radiation are estimated by comparing the nominal  $t\bar{t}W$  prediction with that of an alternative sample that was generated at NLO with the MADGRAPH5\_AMC@NLO 2.2.1 generator using the same scale choice and PDF set as for the nominal sample, and interfaced to PYTHIA 8.2 in combination with the A14 tune. The samples configurations are summarised in Table 2.

#### 3.2 Fiducial Volume

Object and event selection is defined at particle-level that closely matches the detector-level described in reference [2]. Jets are reconstructed from stable particles with a mean lifetime of  $\tau > 3 \times 10^{-11}$  s, using the anti- $k_t$  algorithm with a radius parameter of  $R = 0.4$ . Jets are required to satisfy  $p_T > 25$  GeV and  $|\eta| < 2.5$ . Jets are matched to  $b$ -hadrons with  $p_T > 5$  GeV by ghost matching [17] and are referred to as  $b$ -jets. Electrons and muons, referred to as light leptons, are required to be separated from selected jets by  $\Delta R > 0.4$ . Hadronically decaying  $\tau$  leptons are required to satisfy  $p_T > 25$  GeV and  $|\eta| < 2.5$ . Events are selected with exactly two light leptons. Leptons are required to have  $|\eta| < 2.5$  and  $p_T > 25(20)$  GeV for leading (subleading) lepton. Leptons are required to have same charge, targeting the semi-leptonic  $t\bar{t}$  decay and leptonic  $W$  decay.

Events with at least 3 Jets and least one  $b$ -jet are considered in the fiducial volume. The acceptance for events passing this selection is  $A_X^{\geq 1b \geq 3j} = 1.79 \times 10^{-2}$  for SHERPA and  $1.90 \times 10^{-2}$  for MADGRAPH5\_AMC@NLO correspondingly. We then split into five regions, categorized by the number of jets (three or  $\geq 4$ ),  $b$ -jets (one or  $\geq 2$ ) as well as the presence of hadronically decaying  $\tau$  lepton.

Region 1:  $1 N_{b-jets}, \geq 4 N_{jets}, 0-\tau_{had}$

Region 2:  $\geq 2 N_{b-jets}, \geq 4 N_{jets}, 0-\tau_{had}$

Region 3:  $1 N_{b-jets}, 3 N_{jets}, 0-\tau_{had}$

Region 4:  $\geq 2 N_{b-jets}, 3 N_{jets}, 0-\tau_{had}$

Region 5:  $\geq 1 N_{b-jets}, \geq 3 N_{jets}, 1-\tau_{had}$

### 3.3 Results

The nominal SHERPA  $t\bar{t}W$  sample is compared to its radiation uncertainty variations and the alternative generator. The ratio plot shows the ratio of the alternative MC sample and scale variation to the nominal sample.

Significant discrepancies in the modelling of jet kinematics can be seen between the SHERPA  $t\bar{t}W$  and MADGRAPH5\_AMC@NLO generators in  $1N_{b-jets}$  selections, while in  $\geq 2N_{b-jets}$  the difference is reduced, as illustrated in Figures 7 and 8

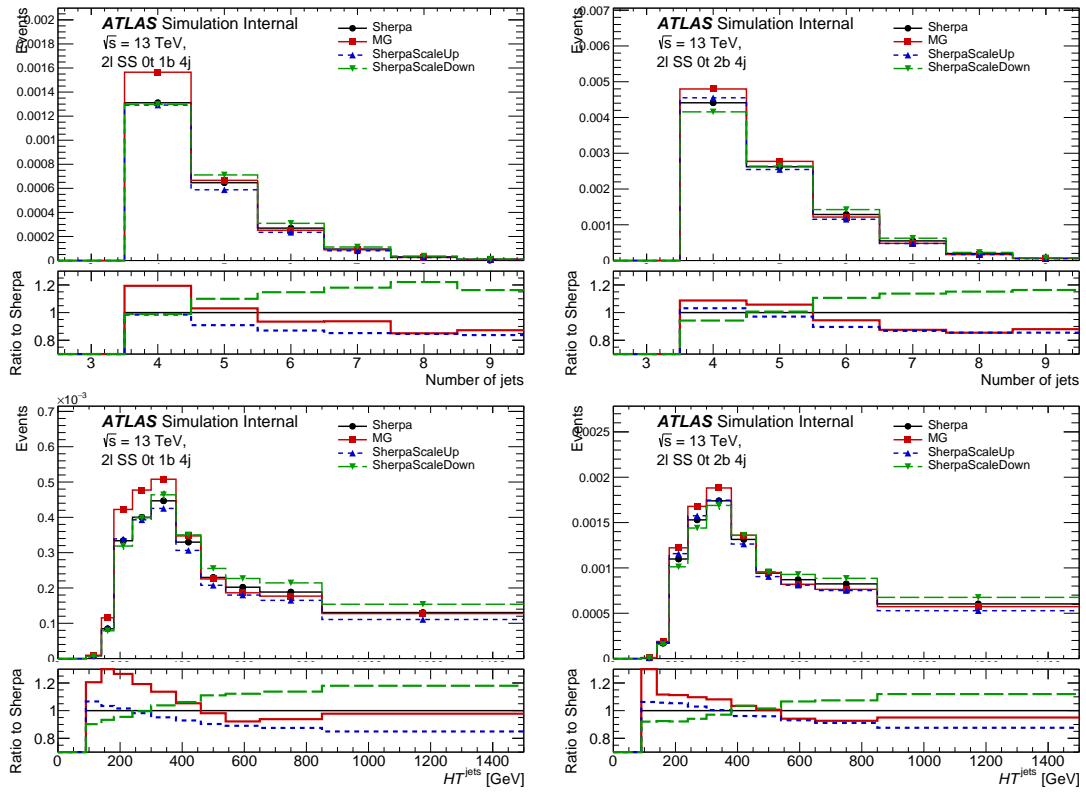


Figure 7: Distribution of the jet multiplicities (top) and the sum of jets transverse momentum,  $HT^{jets}$  (bottom), for the 1b-jet(left) and 2b-jet (right) selection requiring four and more jets. Explanation in text.

Good agreement of the single lepton kinematics can be seen between nominal and alternative generators, as presented in Figures 9. While significant difference in shapes observed for the distributions correlations between two leptons, as illustrated in Figures 10. Distributions are presented for  $\geq 2N_{b-jets}, \geq 4N_{jets}$  region, while similar behaviour seen in all other regions as well.

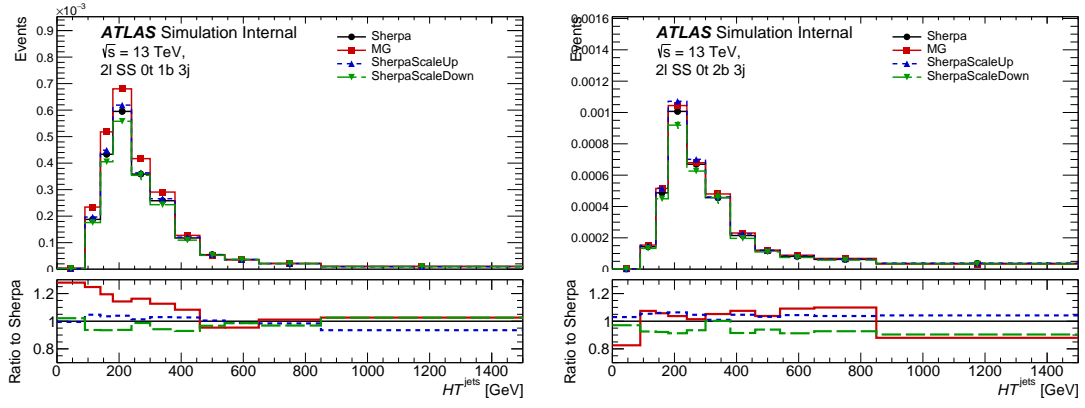


Figure 8: Distribution of the sum of jets transverse momentum,  $HT^{\text{jets}}$ , for the  $1b$ -jet(left) and  $4b$ -jet (right) selection requiring three jets. Explanation in text.

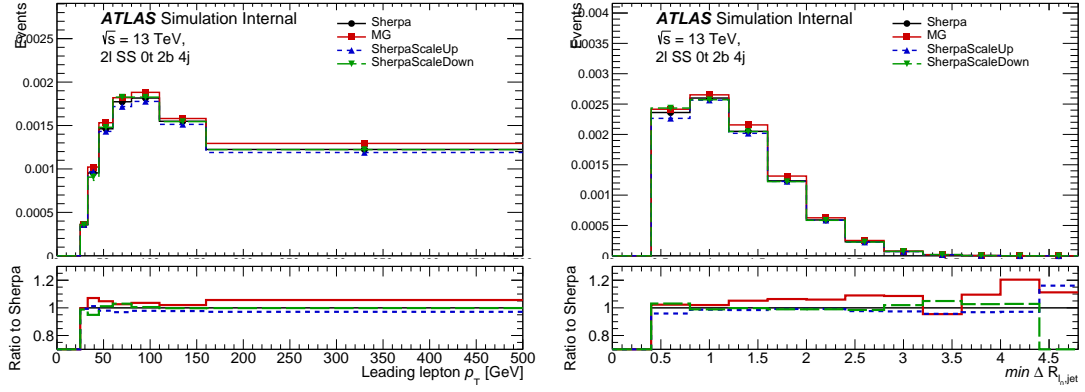


Figure 9: Distribution of the leading lepton transverse momentum (left) and the minimum angular separation between the leading lepton and the nearest jet (right). Explanation in text.

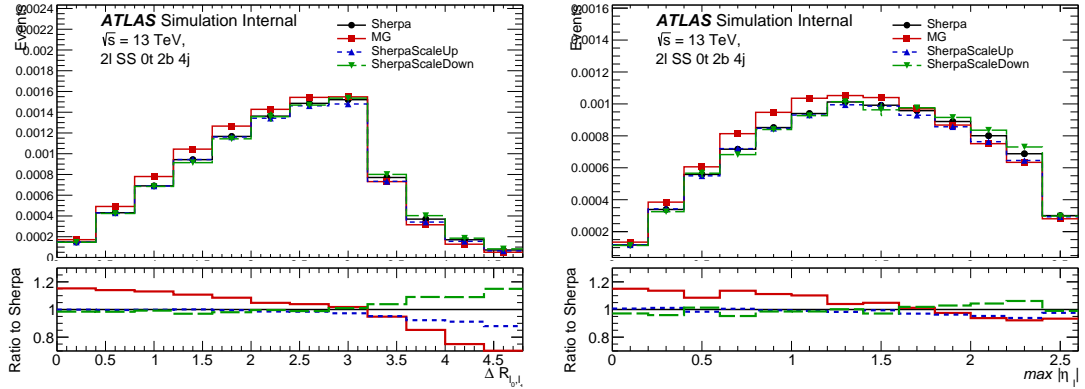


Figure 10: Distribution of the angular distance between the two same-sign lepton (left) and maximum between lepton  $|\eta_{l0}|$  and  $|\eta_{l1}|$  (right). Explanation in text.

## Acknowledgements

In a paper, an appendix is used for technical details that would otherwise disturb the flow of the paper. Such an appendix should be printed before the Bibliography.

## References

- [1] ATLAS Collaboration, *Search for the standard model Higgs boson produced in association with top quarks and decaying into a  $b\bar{b}$  pair in  $pp$  collisions at  $\sqrt{s} = 13$  TeV with the ATLAS detector*, *Phys. Rev. D* **97** (2018) 072016, arXiv: 1712.08895 [hep-ex] (cit. on pp. 3, 4).
- [2] ATLAS Collaboration, *Analysis of  $t\bar{t}H$  and  $t\bar{t}W$  production in the multilepton final states with the ATLAS detector*, ATLAS-CONF-2019-045, 2019, URL: <https://atlas.web.cern.ch/Atlas/GROUPS/PHYSICS/CONFNOTES/ATLAS-CONF-2019-045/> (cit. on pp. 3, 9).
- [3] P. Nason, *A New method for combining NLO QCD with shower Monte Carlo algorithms*, *JHEP* **11** (2004) 040, arXiv: hep-ph/0409146 [hep-ph] (cit. on p. 4).
- [4] S. Frixione, P. Nason and C. Oleari, *Matching NLO QCD computations with Parton Shower simulations: the POWHEG method*, *JHEP* **11** (2007) 070, arXiv: 0709.2092 [hep-ph] (cit. on p. 4).
- [5] S. Alioli, P. Nason, C. Oleari and E. Re, *A general framework for implementing NLO calculations in shower Monte Carlo programs: the POWHEG BOX*, *JHEP* **06** (2010) 043, arXiv: 1002.2581 [hep-ph] (cit. on p. 4).
- [6] J. M. Campbell, R. K. Ellis, P. Nason and E. Re, *Top-Pair Production and Decay at NLO Matched with Parton Showers*, *JHEP* **04** (2015) 114, arXiv: 1412.1828 [hep-ph] (cit. on p. 4).
- [7] ATLAS Collaboration, *Studies on top-quark Monte Carlo modelling for Top2016*, ATL-PHYS-PUB-2016-020, 2016, URL: <https://cds.cern.ch/record/2216168> (cit. on p. 4).
- [8] T. Ježo, J. M. Lindert, N. Moretti and S. Pozzorini, *New NLOPS predictions for  $t\bar{t} + b$ -jet production at the LHC*, *Eur. Phys. J.* **C78** (2018) 502, arXiv: 1802.00426 [hep-ph] (cit. on p. 4).
- [9] D. J. Lange, *The EvtGen particle decay simulation package*, *Nuclear Instruments and Methods in Physics Research Section A: Accelerators, Spectrometers, Detectors and Associated Equipment* **462** (2001) 152, BEAUTY2000, Proceedings of the 7th Int. Conf. on B-Physics at Hadron Machines, ISSN: 0168-9002, URL: <http://www.sciencedirect.com/science/article/pii/S0168900201000894> (cit. on p. 4).
- [10] S. Frixione, E. Laenen, P. Motylinski and B. R. Webber, *Angular correlations of lepton pairs from vector boson and top quark decays in Monte Carlo simulations*, *JHEP* **04** (2007) 081, arXiv: hep-ph/0702198 [HEP-PH] (cit. on p. 4).
- [11] F. Cascioli, P. Maierhöfer, N. Moretti, S. Pozzorini and F. Siegert, *NLO matching for  $t\bar{t}b\bar{b}$  production with massive  $b$ -quarks*, *Phys. Lett.* **B734** (2014) 210, arXiv: 1309.5912 [hep-ph] (cit. on p. 4).
- [12] T. Gleisberg et al., *Event generation with SHERPA 1.1*, *JHEP* **02** (2009) 007, arXiv: 0811.4622 [hep-ph] (cit. on p. 4).
- [13] F. Cascioli, P. Maierhofer and S. Pozzorini, *Scattering Amplitudes with Open Loops*, *Phys. Rev. Lett.* **108** (2012) 111601, arXiv: 1111.5206 [hep-ph] (cit. on pp. 4, 9).

- [14] M. Guzzi et al., *CT10 parton distributions and other developments in the global QCD analysis*, (2011), arXiv: [1101.0561 \[hep-ph\]](#) (cit. on p. 4).
- [15] J. Gao et al., *CT10 next-to-next-to-leading order global analysis of QCD*, *Phys. Rev. D* **89** (2014) 033009, arXiv: [1302.6246 \[hep-ph\]](#) (cit. on p. 4).
- [16] S. Hoeche, F. Krauss, M. Schonherr and F. Siegert, *QCD matrix elements + parton showers: The NLO case*, *JHEP* **04** (2013) 027, arXiv: [1207.5030 \[hep-ph\]](#) (cit. on pp. 4, 9).
- [17] M. Cacciari, G. P. Salam and G. Soyez, *The Catchment Area of Jets*, *JHEP* **04** (2008) 005, arXiv: [0802.1188 \[hep-ph\]](#) (cit. on pp. 4, 9).
- [18] T. Gleisberg et al., *Event generation with SHERPA 1.1*, *JHEP* **02** (2009) 007, arXiv: [0811.4622 \[hep-ph\]](#) (cit. on p. 9).
- [19] T. Gleisberg and S. Hoeche, *Comix, a new matrix element generator*, *JHEP* **12** (2008) 039, arXiv: [0808.3674 \[hep-ph\]](#) (cit. on p. 9).
- [20] S. Schumann and F. Krauss, *A Parton shower algorithm based on Catani-Seymour dipole factorisation*, *JHEP* **03** (2008) 038, arXiv: [0709.1027 \[hep-ph\]](#) (cit. on p. 9).